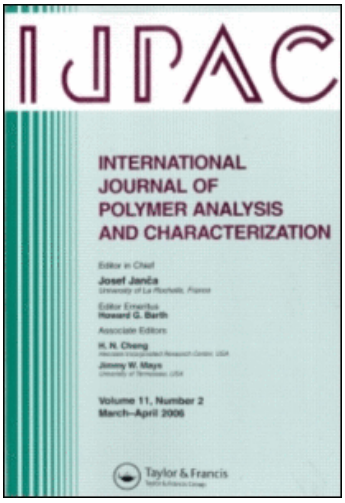

International Journal of Polymer Analysis and Characterization
Publication details, including instructions for authors and subscription information:
http://www.informaworld.com/smpp/title~content=t713646643

Photoaging of Polyoctenamer: Influence of the Initial Microstructure

S. Commereuc[a]; L. Gonon[a]; V. Verney[a]
[a] Laboratoire de Photochimie Moléculaire et Macromoléculaire (UMR CNRS 6505), Groupe Structure-Réactivité des Poolymères, Université Blaise Pascal, Aubière Cedex, France

To cite this Article Commereuc, S. , Gonon, L. and Verney, V.(2000) 'Photoaging of Polyoctenamer: Influence of the Initial Microstructure', International Journal of Polymer Analysis and Characterization, 6: 1, 59 — 74
To link to this Article: DOI: 10.1080/10236660008034650
URL: http://dx.doi.org/10.1080/10236660008034650

Int. J. Polym. Anal. Charact.,
2000 Vol. 6, pp. 59–74
Reprints available directly from the publisher
Photocopying permitted by license only

Photoaging of Polyoctenamer: Influence of the Initial Microstructure*

S. COMMEREUC†, L. GONON and V. VERNEY

Laboratoire de Photochimie Moléculaire et Macromoléculaire (UMR CNRS 6505), Groupe Structure- Réactivité des Poolymères, Université Blaise Pascal, F-63 177, Aubière Cedex, France

(Received 24 September 1999; In final form 12 January 2000)

The photooxidation of two polyoctenamers with different initial microstructures has been investigated through irradiation at $\lambda > 300$ nm at 35°C. Chemical changes were detected using conventional techniques based on FTIR spectroscopy and specific chemical titration. In parallel, the physical evolution was monitored using viscoelastic experiments with the aim of establishing the relationship between chemical and physical changes. Our finding is that the initial microstructure influences the stoichiometric ratio of oxidative byproducts. Moreover, dynamic oscillatory measurements underline an evolution of the molecular structure of the materials from the start of the UV exposure, involving rapid cross-linking. Whereas, at the same time, no chemical change was detected by FTIR spectroscopy. We point out that the physical evolution is independent on the initial microstructure. The critical gel characteristics are quite identical for both samples (gel time $t_{gel} = 125$ min, relaxation exponent $n = 0.4$).

Keywords: Photoaging; Viscoelasticity; FTIR spectroscopy; Cross-linking

INTRODUCTION

Elastomeric materials are especially sensitive to oxidative degradation. Thermooxidation, photooxidation and ozonolysis of such materials have been extensively investigated.[1–13] Recent studies suggested that cross-linking largely controls the photooxidation of

*Presented at the 12th International Symposium on Polymer Analysis and Characterization (ISPAC-12), La Rochelle, France, June 28–30, 1999.

†Corresponding author. Fax: 04-73-40-70-95.

elastomers.[8,9,14–16] However, many of the authors focused their attention on the chemical structure changes detected during the degradation process. Few studies attempt to characterize the three-dimensional network.[17–19] Relationships between the chemical evolution and the physical properties changes of the material are generally not well-known.

We report on the use of the combination of two analytical techniques applied to polyoctenamer photooxidation with the aim of correlating chemical and physical changes. The chemical changes of the material through irradiation at $\lambda > 300$ nm at 35°C are identified by conventional techniques based on FTIR spectroscopy and specific chemical analysis.[13,20–23] In parallel, the physical evolution upon photoaging of the polymer is monitored using melt rheology. The linear viscoelastic properties in a dynamic experiment directly reflect changes in molecular parameters and are especially sensitive to the three-dimensional network formation. Thus, melt rheology provides a convenient method to view the particular behavior of a gelling system.[19]

BACKGROUND

Gelation is the phenomenon by which a cross-linked polymeric material undergoes a phase transition from the liquid to the solid state at a critical point of time, temperature, concentration, *etc.* The sol–gel transition, known as the gel point, occurs at some critical extent of the cross-linking reaction.[24]

Winter and Chambon proposed a general criterion that can be used to identify the gel point. At the gel point, both the elastic modulus G' and the loss modulus G'' exhibit a power-law dependence on the frequency of oscillation ω.[25–28] The corresponding expressions describing dynamic moduli at the gel point are as follows:

$$G'(\omega) = S\Gamma(1-n) \cdot \cos(n\pi/2) \cdot \omega^n \tag{1}$$

$$G''(\omega) = S\Gamma(1-n) \cdot \sin(n\pi/2) \cdot \omega^n \tag{2}$$

The relaxation exponent n can have values in the range $0 < n < 1$, in agreement with previous works in the literature on various model

networks. Thus, at the gel point, the storage and loss moduli depend on the frequency in an identical manner, corresponding to parallel lines in a frequency spectrum

$$G'(\omega) \propto G''(\omega) \propto \omega^n \tag{3}$$

In addition, the loss tangent tan δ becomes independent on the frequency ω, but proportional to the relaxation exponent n

$$\tan\delta = G''/G' = \tan(n\pi/2) \tag{4}$$

The frequency independence of the loss tangent in the vicinity of the gel point has been widely used to determine the gel point of cross-linked polymers.[29-33] Hence, a multifrequencies plot of the loss tangent (tan δ) shows that the values of tan δ converge at the gel point. This method is reliable and valid for the determination of the gel point such as the critical gelation time[29-32] (the irradiation time for us[19]), the degree of cross-linking or the critical gelation concentration.[33]

An alternative way is to plot the "apparent" viscoelastic exponents n' and n'' ($G' \propto \omega^{n'}, G'' \propto \omega^{n''}$), obtained from the approximate scaling laws of the frequency dependence of $G'(\omega)$ and $G''(\omega)$ *versus* irradiation time. In such a manner, curves become congruent and the crossover at $n' = n'' = n$ is an indicator of the gel point.[30,33,34]

Moreover, the evolution of the molecular weight in the pregel regime indicates that the weight-average molecular weight (M_w) increases as the cross-linking reaction proceeds and diverges at the gel point.[21] This property could be used to measure the evolution of an incipient gel near the sol–gel transition. It is well-known that the zero shear viscosity η_0 depends on the molecular weight and obeys a power law[24]

$$\eta_0 \propto M_W^a$$

Thus, at the gel point, the zero shear viscosity becomes infinite and unmeasurable.

The zero shear viscosity η_0 can be obtained from the complex viscosity $\eta^*(\omega)$:

$$\eta^* = G^*(\omega)/i\omega = \eta' - i\eta'' \quad \text{and} \quad |\eta^*|_{\omega\to 0} = |\eta'|_{\omega\to 0} = \eta_0$$

An empirical rheological model used to fit the dynamic data is the Cole–Cole distribution expressed by[35–38]

$$\eta^*(\omega) = \eta_0/[1 + (i\omega\lambda_0)^{1-h}]$$

where λ_0 is the average relaxation time and h the parameter of the relaxation-time distribution.

This model predicts the variation of the viscosity components (η'' *versus* η') to be an arc of circle in the complex plane. Thus, it is easy to determine the parameters of the distribution: η_0 is obtained through the extrapolation of the arc of the circle on the real axis and the distribution parameter h through the measurement of the angle $\Phi = h\pi/2$ between the real axis and the radius going from the origin of the axis to the center of the arc of the circle.

EXPERIMENTAL

Sample Preparation

The polymers used are polyoctenamer rubbers (Vestenamer®) produced by Creanova Company. They possess very low glass-transition temperature, high macrocyclic content, very low viscosity, good compatibility with practically all other types of rubber, thermally reversible crystallinity and high crystallization rate, which lead to extremely interesting application possibilities, especially improved processability of rubber compounds.

Vestenamer® are low-molecular-weight polymers with a broad molecular weight distribution, made from cyclooctene by metathesis polymerization. Polyoctenamer is a member of the general series of polyalkenamers with the repeating unit

$$\sim\!\!\sim\!\!(-CH{=}CH-(CH_2)_6-)\sim\!\!\sim$$

It consists of linear as well as cyclic macromolecules, which are not branched and contain one double bond per eight carbon atoms. The *cis–trans* ratio of the double bonds controls the degree of crystallinity. The molecular characteristics of the two studied polymers are given in Table I.

TABLE I Molecular parameters of Vestenamer®

	M_w	M_n	M_w/M_n	η_0* ($Pa \cdot s$)	% *trans* 1–4	T_m(°C)	ΔH_m(J/g)
V8020	107 400	50 100	2.1	8 300	80	53.0	46.2
V6040	118 900	60 100	2.0	16 000	60	40.7	21.3

* measured at 90°C.

Polymers were precipitated twice from chloroform solution into methanol to remove any additives. The films were prepared by compression molding between two polyester sheets during 1 min at 60°C under 100 bar. The thickness of the films was about 100 μm.

Photooxidation Procedure

The films were fixed on aluminium holders and then irradiated in a polychromatic setup described elsewhere.[13] A "medium-pressure" mercury source filtered by a borosilicate envelope (Mazda type MA 400) supplied radiation of wavelengths greater than 300 nm. This source is located along the focal axis of a cylinder with an elliptical base. Sample films turn around the other focal axis. The inside of the chamber is made of highly reflectant aluminium. The temperature of the samples is controlled by a thermocouple connected with a temperature regulator device that controls a fan. All experiments were carried out at 35°C. The films were analyzed after various exposure times.

Analysis

Chemical changes were detected by FTIR spectroscopy (Nicolet Impact 400, Omnic® software). Total peroxides were estimated by iodometric titration[22,23] based on the reduction of hydroperoxides by sodium iodide in excess in acidic medium according to the reaction

$$ROOH + 2I^- + 2H^+ \rightarrow ROH + I_2 + H_2O$$
$$I_2 + I^- \rightarrow I_3^-$$

The concentration of the triiodide, formed subsequently, is measured by UV spectrophotometry at 362 nm using the commonly accepted extinction coefficient of $2.5\,10^4 mol^{-1} \cdot L \cdot cm^{-1}$.

Rheological Experiments

The changes in dynamic storage G' and loss G'' moduli of photooxidized Vestenamer® were followed in an oscillatory shear mode using a rotational-controlled stress rheometer (StressTech/Rheologica, USA) equipped with a parallel-plate geometry. The plate diameter was 20 mm and the gap between the plates was about 1 mm. In all cases, the values of the stress amplitude were checked to ensure that all measurements were conducted within the linear viscoelastic region. A frequency sweep extending from 0.01 to 30 Hz was performed at different exposure times. Different temperatures have been tested, but the low value of the activation energy involves a small extension of the frequency range. Hence, all experiments were carried out at 90°C. The stability of the oxidized samples at 90°C with respect to the measurement duration has obviously been verified by the reproductibility of the measured moduli.

RESULTS AND DISCUSSION

Chemical Changes Through Photooxidation

Photooxidation of Vestenamer® films leads to significant changes in the IR absorption spectra. Three regions of the spectra examined are

- *Region of hydroxyl stretching vibrations* ($3600-3200\,cm^{-1}$) Figures $1A_1$ and A_2. A broad absorption band centered at $3400\,cm^{-1}$ appears in the first stage of photooxidation. The intensity of this broad band reaches a maximum at $3420\,cm^{-1}$.
- *Region of carbonyl stretching vibrations* ($1830-1600\,cm^{-1}$) Figures $1B_1$ and B_2. First, two absorption bands are observed at 1670 and $1710\,cm^{-1}$. As the exposure time increases, the development of the latter overlaps the former and two additional shoulders are detected at 1730 and $1775\,cm^{-1}$.
- *Region of deformation vibrations* ($1400-600\,cm^{-1}$) Figures $1C_1$ and C_2. IR absorption increases drastically between 1000 and $1400\,cm^{-1}$ with some significant maxima. Each of the out-plane vibrations of C—H linked to unsaturation (*trans* 1–4 at $996\,cm^{-1}$, *cis* 1–4 at $720\,cm^{-1}$) decreases during irradiation.

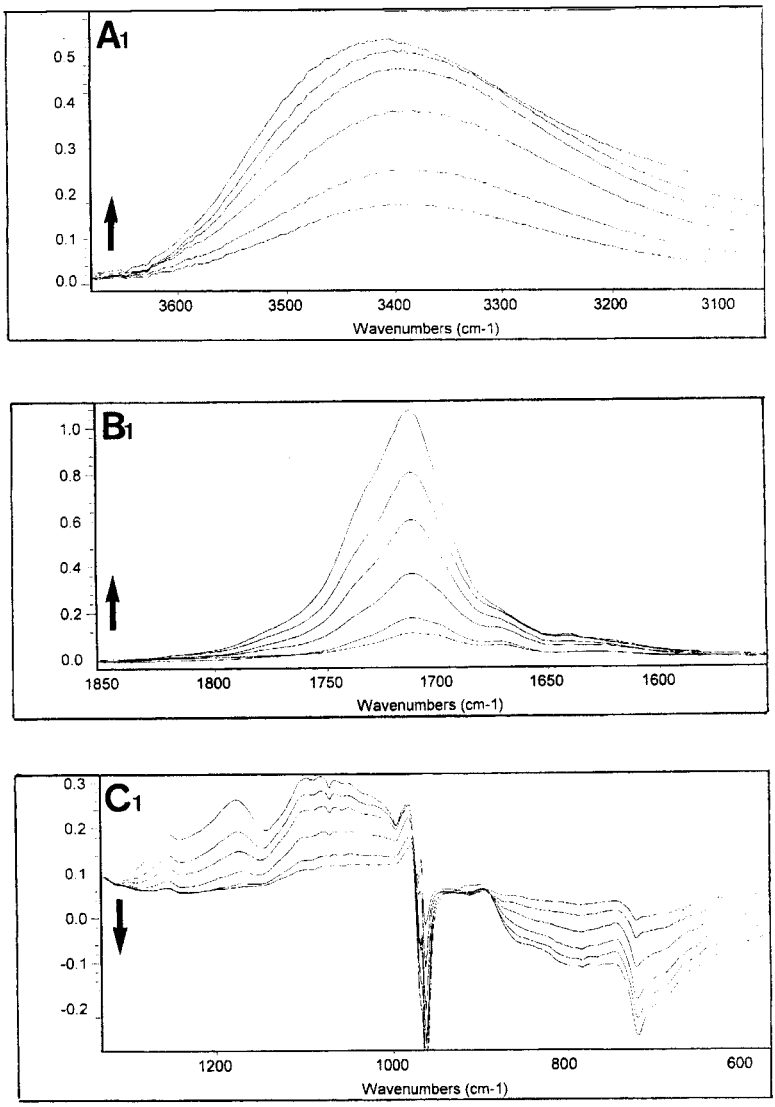

FIGURE 1 FTIR changes upon photooxidation at $\lambda > 300$ nm at 35°C of Vestenamer® films (around 100 μm) for exposure time from 6 to 20 h. Each spectrum was obtained by substracting the non-oxidized from that of the oxidized sample. (1) V8020, (2) V6040. (A) hydroxyl vibration region, (B) carbonyl vibration region, (C) deformation vibration region.

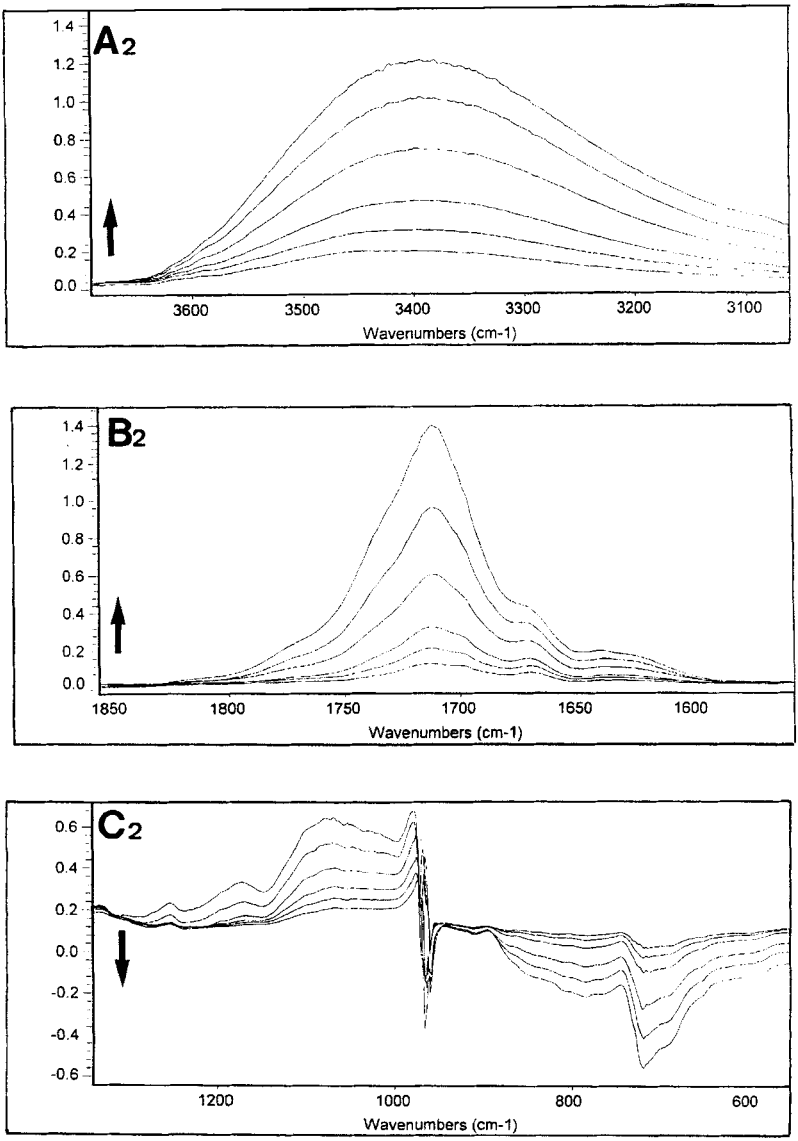

FIGURE 1 (Continued).

Figure 2 shows both kinetic curves of the formation of carbonylated and hydroxylated photoproducts for the two studied polyoctenamers. At the earliest stage of photoageing, no chemical change is detected

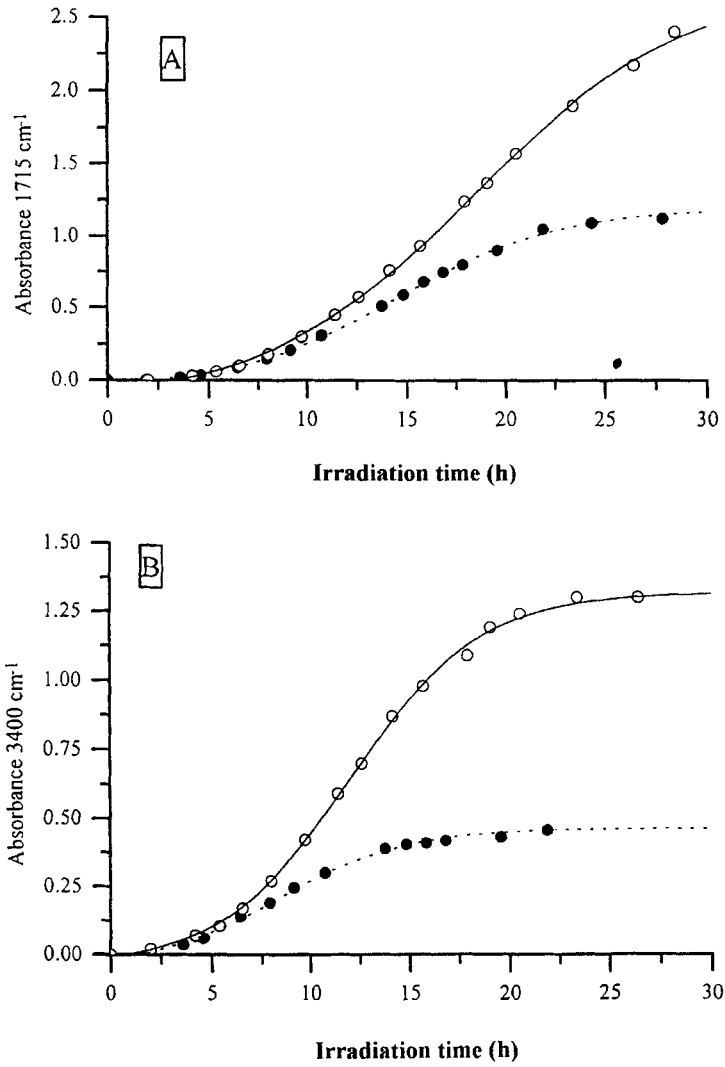

FIGURE 2 Kinetic curves of byproducts from photooxidation at $\lambda > 300$ nm at 35°C of V6040 (open symbols) and V8020 (solid symbols). Films thickness 100 μm. A: hydroxyl absorbance at 3400 cm^{-1}; B: carbonyl absorbance at 1715 cm^{-1}.

by FTIR spectroscopy (irradiation time < 4 h), while iodometric titration reveals a significant content of hydroperoxides rising to a maximum at about 10 h, indicating an evolution of the chemical

structure from the beginning of the irradiation. The results are presented in Table II.

The total hydroperoxide level of the V6040 sample is around 1.7 time higher than that of the V8020, for any exposure time. On the basis of the melting enthalpy values, we can consider that the crystallinity ratio of V6040 is two times lower than that of V8020. Nevertheless, amorphous zones could be reasonably considered as the main probable sites where oxidation takes place. Hence, iodometric titration results could be simply explained.

It is worthwhile to note that the chemical evolution of the two studied samples (V6040 and V8020) exhibits no significant difference in the first stage of the photoaging (until around 7 h of UV exposure). Then, after 10 h of irradiation, the levels and the stoichiometric ratio of oxidation products are different (see Fig. 2).

The mechanism of photooxidation of Vestenamer® involves a primary radical attack on methylene groups in the α-position to a double bond resulting in the formation of α,β unsaturated hydroperoxides which undergo photolysis reactions. Hence, photochemical evolution of Vestenamer® is quite similar to that of other dienic polymers, exhibiting dual processes.[3, 13] In a first stage (irradiation time < 10 h), photooxidation reactions occur implying the formation of hydroperoxides as the primary photoproducts. In a second stage (irradiation time > 10 h), a photolytic process becomes predominant: photooxidation products undergo photolysis reactions. The photolytic decomposition of ROOH prevails and results mainly in the formation of carbonyl groups. Therefore, the high content of ROOH in V6040 simply explains the high level of carbonylated and hydroxylated byproducts detected, especially in the second phase of the photo-aging (photolytic process).

The stoichiometric ratios suggest that hydroxylated species accumulate more readily in the V6040. Several hypotheses, which are

TABLE II Hydroperoxide content (mmol/Kg) from iodometric titration *versus* irradiation time at $\lambda > 300$ nm at 35°C of polycyclooctenamers

Irradiation time	2.5 *h*	8 *h*	10 *h*	11.5 *h*	15 *h*	22.75 *h*	30.5 *h*
V8020	112	328	610	674	380	157	139
V6040	230	604	900	1040	710	416	235

outlined below, are postulated to explain this result:

- *Photostability of hydroperoxides* The high content of ROOH formed in Vestenamer® upon photooxidation could induce associated species by hydrogen links. Hence, the average associated ROOH in V6040 probably differs from that of V8020. However, the stability and the reactivity of isolated and associated ROOH are reported to be different.
- *Molecular mobiliy* affects the photooxidation reaction kinetics. Klyuev *et al.*[39] previously gave an account of the dependence of the kinetics of oxidative degradation on the physical properties of the medium, such as the glass temperature and the viscosity, which are related to molecular motion of polymeric chains.[40] Although the weight-average molecular weights of the two samples V6040 and V8020 are similar, the zero shear viscosity of V6040 is largely higher than that of V8020 (see Tab. I).

Dynamic Viscoelastic Properties Through Photooxidation

Figure 3 displays the complex plane representation of viscosity components through the photooxidation of V6040. The zero shear viscosity η_0 rapidly increases (see Tab. III), and diverges for around 2.5 hours of irradiation. Viscoelastic experiments indicate that the mass-average molecular weight drastically increases (from the increase of η_0) from the very beginning of UV exposure. Thus, no induction period exists. A similar result is obtained from hydroperoxide titration. Elsewhere, the viscosity components curves (η'' *versus* η') rapidly become straight lines as the photooxidation proceeds providing evidence of a tridimensional network formation by cross-linking.

The evolution of the storage G' and loss G'' moduli through photooxidation is quite similar for the two studied samples. Figure 4 shows the storage modulus G' as a function of pulsation ω at different UV exposure time for V6040 sample. The shape of $G'(\omega)$ changes during the irradiation. At around 2 hours of UV exposure, G' shows a power-law variation with respect to the frequency of oscillation ($G' \propto \omega^{n'}$), indicating that the system is in the vicinity of the gel point. As photoaging proceeds, G' increases rapidly and becomes larger than G'', which is a characteristic feature of crosslinked system. The

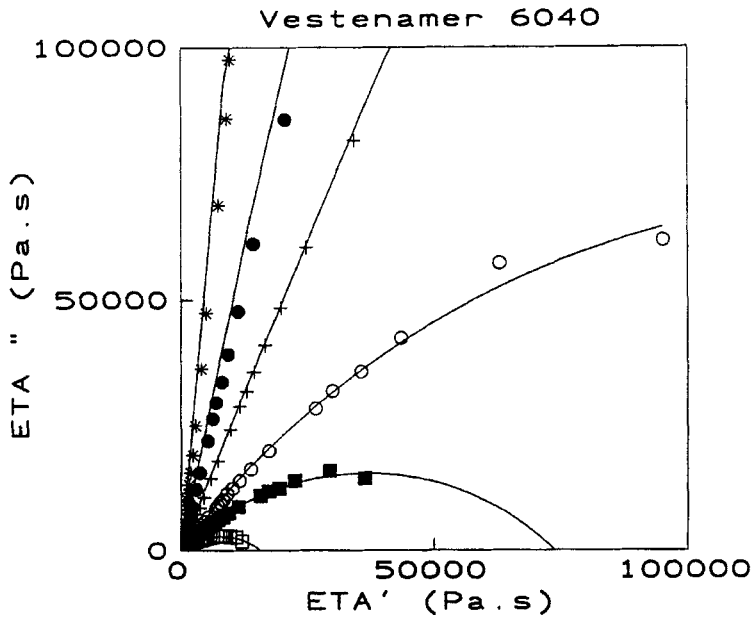

FIGURE 3 Changes of complex viscosity components (η', η'') through photooxidation of V6040 using the Cole–Cole representation; (η'' *versus* η') for different irradiation times: (□) 0h, (■) 1h, (○) 2h, (+) 2.5h, (●) 3h, (*) 5h.

TABLE III Evolution of the zero shear viscosity η_0 (Pa · s) of Vestenamer® through irradiation at $\lambda > 300$ nm at 35°C. Viscosity was measured at 90°C

Irradiation time (h)	*V*8020	*V*6040
0	8 300	16 000
1	18 000	75 000
2	$3.2\ 10^5$	$2.8\ 10^5$
2.5	∞	∞

modulus of the fully crosslinked samples G' appears as frequency independent (at around 5h for V6040, around 10h for V8020).

The evolution of loss modulus G'' is quite similar and not shown. First, G' is always smaller than G'', and both moduli vanish at low frequencies (terminal zone, $G' \propto \omega^2$, $G'' \propto \omega$). Hence, the frequency dependence curves show a liquidlike behavior. Then, as photooxidation proceeds, loss modulus depend on frequency as $G'(G'' \propto \omega^{n'})$. At the gel point, $G''(\omega)$ and $G''(\omega)$ look parallel and $G' \propto G'' \propto \omega^n$.

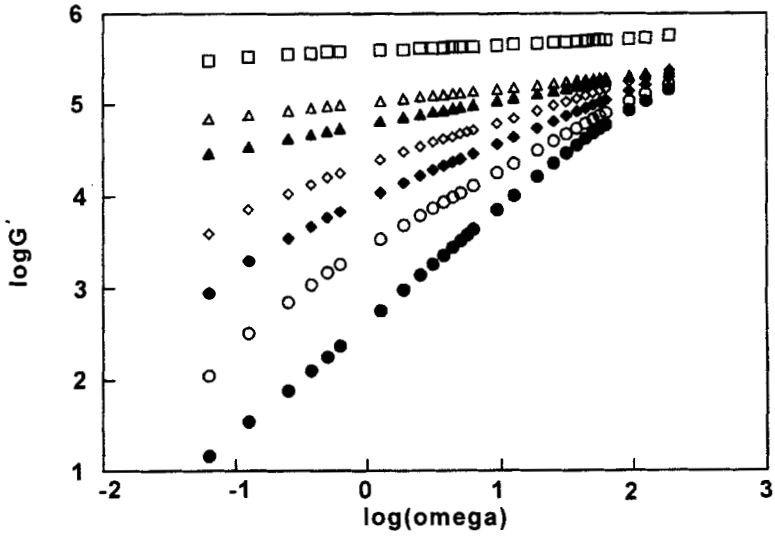

FIGURE 4 Storage modulus G' as a function of frequency pulsation ($\omega = 2\pi N$) plotted at different UV exposure time for V6040 films: (•) 0h, (○) 1 h, (◆) 1.5 h, (◊) 2 h, (Δ) 2.5 h, (Δ) 3 h, (□) 5 h.

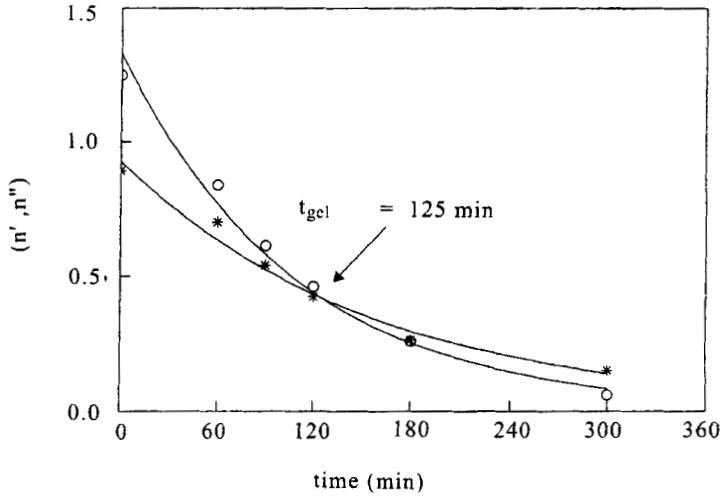

FIGURE 5 Changes of apparent exponents n' (○) for storage and n'' (*) for loss moduli through irradiation of Vestenamer® films (V6040). The notion t_{gel} marks the gel point.

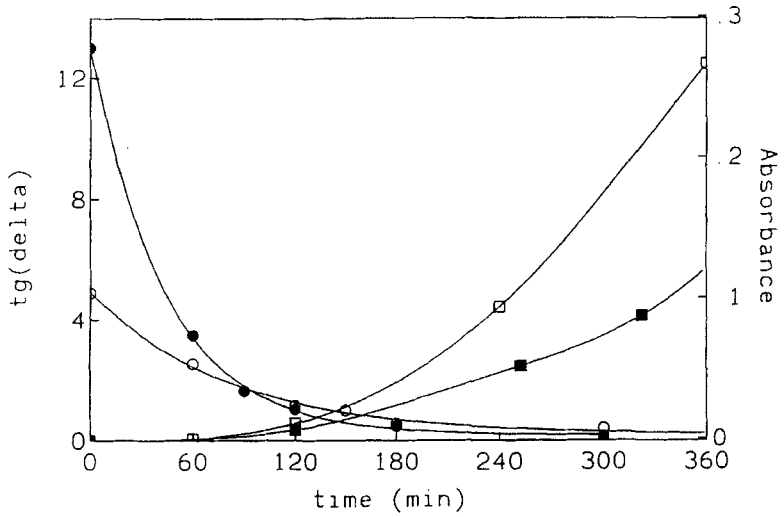

FIGURE 6 Loss angle tangent ($N = 0.04$ Hz, $T = 90°C$) and carbonyl absorbance (film $e = 100\,\mu m$, $1715\,cm^{-1}$) *versus* irradiation time: (open symbols: V8020, closed symbols: V6040).

The gel time (t_{gel}) is accurately determined for the two considered gelling systems obtained from oxidized Vestenamer® (V8020 and V6040).

For the two studied polyoctenamer samples, the values of apparent viscoelastic exponents for both G' and G'' decrease during the irradiation and intersect at an irradiation time $t_{gel} = 125$ mm (illustrated in Fig. 5 for V6040). The critical exponent, $n' = n'' = n$, equals to 0.4. The relaxation exponent depends on the structural and connectivity properties of the incipient gel. The values of t_{gel} and n are quite identical for both V8020 and V6040. As a result, we assume that the two studied materials (V6040 and V8020) are fully cross-linked when the carbonylated photoproducts are clearly detected by FTIR spectroscopy (see Fig. 6).

CONCLUSION

Compared with conventional techniques, viscoelastic measurements give additional information concerning molecular structure evolution

involving cross-linking. Indeed, chemical analysis cannot reveal network formation through photoaging, but can identify subsequent photoproducts. We assume that melt rheology is a powerful tool (easy, accurate and very sensitive) to monitor the molecular structure evolution of the material through aging and it provides an accurate diagnosis about gelation phenomenon, cross-linking extent and critical gel characterization. In the case of elastomers, gelation occurs at the very beginning of the UV exposure, and, the material is readily fully cross-linked when photoproducts are detected by FTIR spectroscopy.

It is worthwhile to note that this gelation phenomenon appears to be independent on the initial microstructure of the polyoctenamer, while the chemical changes are readily different probably arising from different crystallinity degrees.

References

[1] S. W. Beavan and D. Philips (1974). *Fur. Polym. J.*, **10**, 593.
[2] J. Lacoste, C. Adam, N. Siampiringue and J. Lemaire (1994). *Eur. Polym. J.*, **30**, 443.
[3] M. Piton and A. Rivaton (1997). *Polym. Degrad. Stab.*, **55**, 147.
[4] K. W. Ho (1986). *J. Polym. Sci.*, **24**, 2467.
[5] R. L. Pecsok, J. R. Shelton and J. L. Koenig (1981). *Rubber Chem. Technol.*, **49**, 324.
[6] S. Yano (1980). *Rubber Chem. Technol.*, **54**, 1.
[7] J. Lucki, B. Ranby and J. F. Rabek (1979). *Eur. Polym. J.*, **15**, 1089, see also 1107.
[8] C. Adam, J. Lacoste and J. Lemaire (1989). *Polym. Degrad. Stab.*, **24**, 185.
[9] C. Adam, J. Lacoste and J. Lemaire (1990). *Polym. Degrad. Stab.*, **29**, 305.
[10] C. Adam, J. Lacoste and J. Lemaire (1989). *Polym. Degrad. Stab.*, **26**, 269.
[11] C. Adam, J. Lacoste and J. Lemaire (1990). *Polym. Degrad. Stab.*, **27**, 85.
[12] C. Adam, J. Lacoste and J. Lemaire (1991). *Polym. Degrad. Stab.*, **32**, 51.
[13] S. Commereuc and J. Lacoste (1997). *Polym. Degrad. Stab.*, **57**, 31.
[14] M. A. De Paoli (1983). *Eur. Polym. J.*, **19**, 761.
[15] L. Audouin, V. Langlois, J. Verdu and J. C. De Bruijn (1994). *J. Mater. Sci.*, **29**, 569.
[16] R. L. Clough and K. T. Gillen (1992). *Polym. Degrad. Stab.*, **38**, 47–56.
[17] C. Adam, J. Lacoste and G. Dauphin (1991). *Polym. Commun.*, **32**(10), 317.
[18] M. Baba (1999). *Polym. Degrad. Stab.*, **63**(1), 121.
[19] S. Commereuc, S. Bonhomme, V. Verney and J. Lacoste (2000). *Polymer*, **41**, 917.
[20] D. J. Carlsson, R. Brousseau, C. Zhang and D. Wiles (1988). *Am. Chem. Soc., Symp. Ser.*, **364**, 376.
[21] C. Wilhem and J. L. Gardette (1994). *J. Appl. Polym. Sci.*, **51**, 1411.
[22] D. J. Carlsson and J. Lacoste (1991). *Polym. Degrad. Stab.*, **32**, 377.
[23] J. Scheirs, D. J. Carlsson and S. W. Bigger (1995). *Polym.-Plast. Technol. Eng.*, **34**(1), 97.
[24] H. H. Winter (1989). Gel Point, In: *Encyclopedia of Polymer Science and Engineering*, John Wiley & Sons, New-York.

[25] F. Chambon and H. H. Winter (1985). *Polym. Bull.*, **13**, 499.
[26] H. H. Winter and F. Chambon (1986). *J. Rheol.*, **30**, 367.
[27] F. Chambon and H. H. Winter (1987). *J. Rheol.*, **31**, 683.
[28] S. K. Venkaraman and H. H. Winter (1990). *Rheol. Acta*, **29**, 423.
[29] I. Espinasse, P. Cassagnau, M. Bert and A. Michel (1994). *J. Appl. Polym. Sci.*, **54**, 2083.
[30] A. Kjoniksen and B. Nyström (1996). *Macromolecules*, **29**, 5215.
[31] J. P. Eloundou, M. Feve, J. F. Gerard, D. Harran and J. P. Pascault (1996). *Macromolecules*, **29**, 6907.
[32] B. Chiou, R. J. English and S. K. Khan (1996). *Macromolecules*, **29**, 5368.
[33] L. Li and Y. Aoki (1997). *Macromolecules*, **30**, 7835.
[34] D. F. Hogdsgon and E. J. Amis (1991). *Non-Cryst. Solids*, **131–133**, 913.
[35] V. Verney and M. Michel (1986). *Rheol. Acta*, **24**(6), 627.
[36] V. Verney and M. Michel (1989). *Rheol. Acta*, **28**, 54.
[37] J. F. Vega, A. Munoz-escalona, A. Santamaria, M. E. Munoz and P. Lafuente (1996). *Macromolecules*, **29**, 960.
[38] J. P. Montfort, G. Mann and P. Monge (1984). *Macromolecules*, **17**, 1551.
[39] A. Yu. Klyuev, R. G. Shlyashinskii, A. A. Erdman, N. R. Prokopchuk and E. I. Vecher (1995). *Russian J. Appl. Chem.*, **68**/**6**(2), 879–883.
[40] M. L. Binet, S. Commereuc and V. Verney (1999). *Fur. Polym. J.*, in press.